

A Novel Generalized Metaheuristic Framework for Dynamic Capacitated Arc Routing Problems

Hao Tong^{1b}, *Member, IEEE*, Leandro L. Minku^{2b}, *Senior Member, IEEE*, Stefan Menzel^{3b},
Bernhard Sendhoff^{4b}, *Fellow, IEEE*, and Xin Yao^{5b}, *Fellow, IEEE*

Abstract—The capacitated arc routing problem (CARP) is a challenging combinatorial optimization problem abstracted from many real-world applications, such as waste collection, road gritting, and mail delivery. However, few studies considered dynamic changes during the vehicles' service, which can cause the original schedule infeasible or obsolete. The few existing studies are limited by the dynamic scenarios considered, and by overly complicated algorithms that are unable to benefit from the wealth of contributions provided by the existing CARP literature. In this article, we first provide a mathematical formulation of dynamic CARP (DCARP) and design a simulation system that is able to consider dynamic events while a routing solution is already partially executed. We then propose a novel framework which can benefit from the existing static CARP optimization algorithms so that they could be used to handle DCARP instances. The framework is very flexible. In response to a dynamic event, it can use either a simple restart strategy or a sequence transfer strategy that benefits from the past optimization experience. Empirical studies have been conducted on a wide range of DCARP instances to evaluate our proposed framework. The results show that the proposed framework significantly improves over state-of-the-art dynamic optimization algorithms.

Index Terms—Dynamic capacitated arc routing problem (DCARP), experience-based optimization, metaheuristics, restart strategy (RS), transfer optimization.

Manuscript received 13 April 2021; revised 3 September 2021 and 29 November 2021; accepted 12 January 2022. Date of publication 31 January 2022; date of current version 1 December 2022. This work was supported in part by the Honda Research Institute Europe (HRI-EU); in part by the Guangdong Provincial Key Laboratory under Grant 2020B121201001; in part by the Program for Guangdong Introducing Innovative and Entrepreneurial Teams under Grant 2017ZT07X386; in part by the Shenzhen Science and Technology Program under Grant KQTD2016112514355531; in part by the Guangdong Basic and Applied Basic Research Foundation under Grant 2021A1515011830; and in part by the Research Institute of Trustworthy Autonomous Systems (RITAS). The work of Hao Tong was supported by the Honda Research Institute Europe (HRI-EU). (*Corresponding author: Xin Yao.*)

Hao Tong is with the School of Computer Science, University of Birmingham, Birmingham B15 2TT, U.K. (e-mail: hxt922@cs.bham.ac.uk).

Leandro L. Minku is with the School of Computer Science, University of Birmingham, Birmingham B15 2TT, U.K. (e-mail: l.l.minku@cs.bham.ac.uk).

Stefan Menzel and Bernhard Sendhoff are with the Honda Research Institute Europe GmbH, 63073 Offenbach, Germany (e-mail: stefan.menzel@honda-ri.de; bernhard.sendhoff@honda-ri.de).

Xin Yao is with the School of Computer Science, University of Birmingham, Birmingham B15 2TT, U.K., and also with the Department of Computer Science and Engineering, Research Institute of Trustworthy Autonomous Systems, Southern University of Science and Technology, Shenzhen 518055, China (e-mail: xiny@sustech.edu.cn).

This article has supplementary material provided by the authors and color versions of one or more figures available at <https://doi.org/10.1109/TEVC.2022.3147509>.

Digital Object Identifier 10.1109/TEVC.2022.3147509

I. INTRODUCTION

THE CAPACITATED arc routing problem (CARP) is a classical combinatorial optimization problem with a range of collection and delivery applications in the real world. For example, in a waste collection problem [1], the capacitated vehicles start from a depot to collect the waste distributed in different streets. In a winter road gritting problem, which is a kind of delivery application [2], the fully loaded vehicles deliver the salt to spread into different required roads. Such scenarios are the main focus in this article.

Constructive heuristic methods, such as Ulusoy's split [3] and Path-Scanning [4], were proposed to construct feasible executable solutions for CARP based on an optimized sequence of tasks. Tabu search [5], memetic algorithms [6], and others were also proposed to solve the CARP. In addition, efficient algorithms have been proposed to tackle large-scale CARPs [7], [8]. Many different variants of CARP have been investigated [9], [10]. For example, multidepot CARP considers several different depots in the graph [11], and open CARP allows the routes to be open with different starting and ending nodes [12]. Split-delivery CARP allows the edge demand to be served by several vehicles [13]. Periodic CARP considers the cases where the tasks are required to be served with a certain number of times over a given multiperiod horizon [14]. Time CARP considers the time instead of the volume restriction of the vehicles [15].

However, all these studies concentrate on static CARPs, where the problem remains static during the entire time of a solution's execution. In real applications, dynamic changes usually happen when vehicles are in service, i.e., when a solution is partially executed, thus influencing the vehicles' follow-on service. For example, a road may be closed due to an accident or new tasks may emerge during the vehicles' service. When that happens, a new graph, i.e., a new problem instance, is formed, in which vehicles would stop at different locations, labeled as outside vehicles, with various amounts of remaining capacities. As a result, the current schedule may become inferior or even infeasible. Dynamic CARP (DCARP) in our article thus aims at rescheduling the service plan [16], [17]. For clarity, the following three different concepts are used throughout our article.

- 1) *DCARP*: A variant of CARP where the status of a graph is changed due to dynamic events occurring during a CARP solution's execution.
- 2) *DCARP Instance*: The updated graph with some outside vehicles after the dynamic events happen.

- 3) *DCARP Scenario*: A scenario contains a series of DCARP instances with the whole service process, starting from executing an initial solution in the original CARP map until all tasks are served.

It is worth noting that Mei *et al.* [18] used the term DCARP to denote the uncertain CARP, which is different from the meaning of DCARP in this article. Uncertain CARP focuses on robust optimization [18], [19], where one is interested in finding solutions that are *robust* to uncertainties, such as changing degrees of congestion or level of demands. However, there are dynamic events in the real world which cannot be handled well by robust optimization, such as the closure of roads or addition of new tasks. As a result, dynamic optimization, which is the focus of our article, has been an active research topic in recent years.

DCARP, as we defined early, was first investigated in [20] when considering the salting route optimization problem. However, few studies in the literature have focused on DCARP so far. Tagmouti *et al.* [21] solved DCARP with time-dependent service costs motivated from winter gritting applications. Liu *et al.* [16] defined some dynamics in DCARP and proposed a benchmark generator for DCARP [17]. Monroy-Licht *et al.* [22] dealt with rescheduling for DCARP, which considered the failure of vehicles. Padungwech *et al.* [23] considered new tasks in DCARP. A robot path planning problem [24] and our previous work [25] focused on the split scheme in DCARP. Split schemes convert an ordered task sequence into an executable solution of multiple explicit routes.

Even though DCARP has been investigated by different people, there is still a lack of formal mathematical formulation of DCARP to the best of our knowledge. The field also lacks a system that can simulate the behavior of vehicle's service process in the real world. Liu *et al.* [17] proposed a benchmark generator for DCARP. However, their generator cannot consider dynamic events during the execution of a routing solution and, thus, is unsuitable for our DCARP scenarios, where changes happen during the execution of the scenarios. Finally, there is a rich literature on existing CARP optimization algorithms that could potentially contribute toward DCARP optimization, but they are not applicable to DCARP instances. This is because they work under the assumption that all vehicles start at the depot and have the same capacities, which is not the case in DCARP. A framework to enable the application of the existing CARP optimization algorithms to DCARP problems is desirable.

Therefore, this article has the following contributions.

- 1) We provide the first mathematical formulation of DCARP in the literature.
- 2) We design a simulator to simulate the behavior of vehicles' service processes in the real world. The simulator is developed according to the collection or gritting problem, where the vehicle does not have to return to the depot for loading new different delivered items. It offers a novel research platform to support DCARP studies.
- 3) We propose a novel framework capable of generalizing almost all existing algorithms designed for static CARP

to the DCARP context. The framework converts a DCARP instance into a "static" CARP instance by introducing the idea of "virtual tasks" (VTs), which enables outside vehicles (with potentially partial capacity) to be interpreted as vehicles located at the depot (with their full capacity). The DCARP instance can then be solved as if it was a static CARP instance by static CARP algorithms. After a solution is found, its corresponding DCARP route where the vehicles start at their outside positions is generated.

- 4) As a dynamic scenario is composed of a series of DCARP instances, similarities between DCARP instances can and should be exploited. Therefore, we propose two strategies for generating initial solutions in our framework, namely, a *sequence transfer strategy* (STS) and a *restart strategy* (RS), to solve a new DCARP instance. The STS generates a potentially good solution based on the previous optimization experience by transferring the sequence of remaining unserved tasks. The RS starts from scratch without using any information and optimizes each DCARP instance independently of each other.
- 5) We perform extensive experiments with a variety of DCARP instances, demonstrating the effectiveness of the proposed framework. We show that valuable research progress achieved by the static CARP literature can contribute toward optimization results that significantly outperform the existing algorithm [16] that was specifically designed for DCARP.

The remainder of this article is organized as follows. Section II discussed the related work on DCARP and this article's motivation. After that, a general mathematical formulation of DCARP and a simulation system for DCARP are provided in Section III. Section IV introduces the main algorithm of our generalized optimization framework for DCARP. Section V presents our experimental study on the proposed framework to evaluate its efficiency. Section VI concludes this article.

II. RELATED WORK AND MOTIVATION

In the literature, there are two related but different research topics, which target the (re)scheduling of vehicles in dynamic environments: 1) DCARP and 2) dynamic vehicle routing problem (DVRP). DCARP focuses on serving tasks, which are the arcs in the graph while DVRP focuses on serving vertices. With respect to DCARP, few approaches were proposed. Liu *et al.* [16] proposed a memetic algorithm with a new distance-based split scheme (MASDC) for DCARP. However, its performance is unsatisfactory since it suffers from noise in the fitness evaluation due to the impact of random splits, as well as the neglecting available vehicles placed in the depot. Monroy-Licht *et al.* [22] considered only the broken down vehicles and presented a heuristic to minimize the operations and disruption cost. Padungwech *et al.* [23] considered only the new tasks during the vehicles' service. They applied the tabu search to optimize the DCARP, in which the solution is represented as routes with different start vertices.

As stated above, DVRP focuses on serving vertices, instead of tasks/arcs (i.e., arcs with demands), and its research work mainly comprises two categories called dynamic deterministic VRP and stochastic VRP according to if problem knowledge is used during the optimization or not [26]. For solving DVRP, it might be possible to transform DVRP instances into DCARP instances or vice versa, such transformation will increase the problem's dimension [27]. For example, the number of vertices in the capacitated VRP (CVRP) instance will increase if transformed from a CARP instance. The number of vertices to be served will be greater than the number of arcs to be served. Furthermore, dynamics events in VRP and CARP are very different. In short, it is not a suitable approach to convert CARP into CVRP and then solve CVRP. It is better to design CARP or DCARP specific algorithms as the research community has been doing for many years.

There are two representations commonly used in optimization algorithms for CARP in the literature. The first type provides all explicit routes in the solution, separated by a dummy task [6], while the other type is an ordered list of tasks without separation. These two types of representation can be used together in the algorithm for CARP. For example, constructive heuristics, such as Path-Scanning [4] generates solutions with explicit routes. This representation is friendly to local search operator. The representation with an ordered list of tasks is often used in metaheuristic algorithms with crossover operators, such as memetic algorithms [1], [6]. Ulusoy's split scheme [3] is an exact algorithm for converting an ordered list of tasks to a solution with explicit routes by building an auxiliary graph according to the task sequences.

For DCARP, the calculation of the cost and capacity violation of the routes corresponding to the outside vehicles are required to be specifically considered due to the fact that outside vehicles have different locations and remaining capacities. It is more complicated to use an ordered list of tasks as the solution representation during the optimization because Ulusoy's split [3] is not suitable anymore and specific split schemes [25] are required. Even though a new split scheme was proposed in our previous work [25], its high computational complexity limits its performance. Therefore, the existing algorithm for static CARP [16] is adapted to solve DCARP instance with some modification, such as the existing work in [16].

In this article, we propose a novel general framework, which enables the adoption of existing CARP algorithms to DCARP. However, this does not exclude future development of new dedicated dynamic algorithms. In the next section (Section III), we will introduce our mathematical formulation of DCARP and a newly designed simulation system, followed by our general framework in Section IV.

III. PROBLEM FORMULATION AND SIMULATION SYSTEM

In this section, we provide the first mathematical formulation for DCARP. The mathematical notations used in this article are summarized in Table I. A new simulation system is then proposed to generate benchmark instances from the existing CARP benchmark for testing DCARP algorithms.

TABLE I
GLOSSARY OF MATHEMATICAL NOTATIONS USED IN THIS ARTICLE

Symbols	Meaning
G	Graph $G = (V, A)$
V	Set of vertices.
A	Set of arcs.
I_m	The m^{th} DCARP instance.
v_0	The depot.
$dm(u)$	The demand of an arc $u \in A$ (ID).
$dc(u)$	The deadheading(traversing) cost of an arc $u \in A$ (ID).
$sc(u)$	The serving cost of an arc $u \in A$ (ID).
$state(u)$	The traffic property of an arc $u \in A$ (ID).
N_t	The number of tasks, $N_t = R $.
N_{veh}	The maximum number of vehicles.
Q	The capacity of empty vehicles.
OV	The set of outside vehicles.
N_{ov}	The number of outside vehicles, $N_{ov} = OV $.
q_k	The remaining capacity of the k^{th} outside vehicle.
$mdc(v_i, v_j)$	The minimal total deadheading cost from vertex v_i to v_j .
$head_t$	The head node of task t .
$tail_t$	The tail node of task t .
S	A DCARP solution, i.e., a set of routes.
r_k	The k^{th} route.
l_k	The number of tasks in k^{th} route.
$t_{k,i}$	The i^{th} task in k^{th} route.
RC_{r_k}	The total cost of k^{th} route r_k .
$TC(S)$	The total cost of solution S .

The set of outside vehicles OV depends on the dynamic changes that different changes at different times will lead to different OV .

A. Notations and Mathematical Formulation

For simplicity, in the present article, we consider the collection or gritting application, i.e., vehicles can continue the service paths without requiring to return to the depot when new tasks/demands appear. Such a DCARP scenario is composed of a series of DCARP instances: $\mathcal{I} = \{I_0, I_1, \dots, I_m, \dots, I_M\}$. Each DCARP instance corresponds to a problem state, which contains all the information regarding the state of the map and vehicles involved in the routing problem, and highly depends on the previous instance and the solution's execution. The initial problem instance I_0 is a conventional static CARP, in which all vehicles are located at the depot having the same full capacities. We can obtain an initial solution in I_0 and execute this solution in the graph. During the execution, some dynamics [16] happen at random points in time when vehicles are in service, thus changing the problem instance and potentially requiring a new better solution. Vehicles then continue to serve tasks from the positions they had stopped (stop points). DCARP terminates when all tasks are served, and all vehicles have returned to the depot. In a DCARP scenario, the key objective is to achieve a schedule cost, which should be as low as possible for each DCARP instance. Let us first focus on the mathematical formulation for one DCARP instance.

The map for any DCARP instance I_m is provided as a graph G . Suppose the map of a DCARP instance I_m is represented by $G = (V, A)$ with a set of vertices V and arcs (directed links) A . There is a depot $v_0 \in V$ in the graph, which contains vehicles that are not yet serving any tasks. Set A is given by

$$A = \{ \langle v_i, v_j \rangle \mid v_i, v_j \in V \}$$

where for each arc u , i.e., $\langle v_i, v_j \rangle \in A$, v_i is the head vertex and v_j is the tail vertex. A given arc $\langle v_i, v_j \rangle$ only

exists if it is possible to traverse from vertex v_i to vertex v_j without passing through other vertices. Each arc u in the graph is associated with a deadheading (traversing) cost $dc(u)$, a serving cost $sc(u)$ and a demand $dm(u)$. The deadheading cost of an arc means the cost that the vehicle just traverse this arc without serving while the serving cost is the cost when vehicles serve this arc. For simplicity, the deadheading cost is assumed to be symmetric in this article. The deadheading cost has been included in the serving cost such that the deadheading cost is not required to be calculated when the vehicle serves an arc. A subset $R \subseteq A$ contains all arcs required to be served in the graph. The arc $u \in R$ is named as ‘‘task’’ and has a positive demand $dm(u) > 0$. For convenience, we use t to represent a task, and use an arc ID for identification.

The DCARP instance I_0 only contains vehicles at the depot. As for DCARP instances $I_m (m > 0)$, in addition to vehicles that are currently at the depot, there may also be outside vehicles with remaining capacities. These are vehicles that had already started to serve tasks when a dynamic event occurs. Suppose there are N_{veh} vehicles in total with a maximum capacity Q at the depot and N_{ov} ($N_{ov} \leq N_{veh}$) outside vehicles with remaining capacities $\{q_1, q_2, \dots, q_{N_{ov}}\}$. The stop points (locations) of the outside vehicles are labeled as $OV = \{v_1, v_2, \dots, v_{N_{ov}}\}$. The optimization of DCARP aims to reschedule the remaining tasks with the minimal cost considering both outside and depot vehicles..

A DCARP solution $S = \{r_1, r_2, \dots, r_{N_{ov}}, \dots, r_K\}$ contains K routes, where the routes r_1 to $r_{N_{ov}}$ start from locations that outside vehicles located while routes $r_{N_{ov}+1}$ to r_K start from the depot. Each route can be represented by three components: 1) starting vertex; 2) an ordered list of tasks (arc IDs); and 3) the final depot. Therefore, a given route r_k can be expressed as $r_k = (v_k, t_{k,1}, t_{k,2}, \dots, t_{k,l_k}, v_0)$, where the vehicle starts from stop location v_k and returns to the depot v_0 , whereas l_k denotes the number of tasks served by route r_k . For route r_k , where $k > N_{ov}$, v_k equals v_0 . This representation is very easy to be converted to an explicit route by connecting two subsequent tasks using Dijkstra’s algorithm so that the route cost can be calculated. In addition, a DCARP solution has to satisfy the following three constraints which are the same as constraints in static CARP.

- 1) Each route served by one vehicle must return to the depot.
- 2) Each task has to be served once.
- 3) The total demand for each route served by one vehicle cannot exceed the vehicle’s capacity Q .

Due to the different remaining capacities for outside vehicles, the capacity constraint is required to be formulated for each outside vehicle separately. As a result, the objective function and the constraints for DCARP are given as follows:

$$\begin{aligned} \mathbf{Min} \quad & TC(S) = \sum_{k=1}^K RC_{r_k} \\ \mathbf{s.t.} \quad & \sum_{k=1}^K l_k = N_t \\ & t_{k_1, i_1} \neq t_{k_2, i_2}, \text{ for all } (k_1, i_1) \neq (k_2, i_2) \end{aligned}$$

$$\begin{aligned} \sum_{i=1}^{l_k} dm(t_{k,i}) &\leq q_k \quad \forall k \in \{1, 2, \dots, N_{ov}\} \\ \sum_{i=1}^{l_k} dm(t_{k,i}) &\leq Q \quad \forall k \in \{N_{ov} + 1, \dots, K\} \end{aligned} \quad (1)$$

where N_t is the number of tasks and RC_{r_k} denote the total cost of route r_k and is computed according to

$$\begin{aligned} RC_{r_k} &= mdc(v_k, tail_{t_{k,1}}) + mdc(head_{t_{k,l_k}}, v_0) \\ &+ \sum_{i=1}^{l_k-1} mdc(head_{t_{k,i}}, tail_{t_{k,i+1}}) + \sum_{i=1}^{l_k} sc(t_{k,i}) \end{aligned} \quad (2)$$

where $head_t$ and $tail_t$ denote the head and tail vertices of the task, $mdc(v_i, v_j)$ denotes the minimal total deadheading cost traversing from node v_i to node v_j , and $sc(t_{k,i})$ denotes the serving cost of task $t_{k,i}$. The first two constraints in (1) guarantee that all tasks are served only once and the other two constraints are formulated to satisfy the capacity constraint.

B. Simulation System for DCARP

In order to test optimization algorithms for DCARP, a simulation system that includes some common dynamic events is required. Even though a benchmark generator for DCARP has been proposed by Liu *et al.* [17], it has shortcomings, which prevent it to be used as the research platform. Intuitively, a DCARP instance should be generated from the dynamic change of a previous DCARP instance during a solution’s execution, such as road congestion or recovering from the congestion. However, these essential details are not considered in the existing benchmark generator [17]. Therefore, we have designed a simulation system which includes nine commonly occurring events and generates DCARP instances from the existing CARP benchmark.¹ Nine events and their corresponding changes in mathematical forms are listed in Table II, and the simulation system’s architecture is presented in Fig. 1.

To make our simulator more close to realistic events, we have added several dynamic events, which have not been considered in the literature. For example, the road can recover from a closure or a congestion, which has been marked with a star (*) in Table II. If a vehicle breaks down, we can assume that this vehicle k has already served some tasks. Consequently, the demand of arc u_k , where vehicle k broke down, increases from 0 to $Q - q_k$ to include the already served loads in collection applications. For delivery applications, the broken down vehicle has no impact to the demand of the arc. As we mainly considered collection or gritting problems, we assumed in our work that the tasks/demands will not vanish until fully served, although this may be extended and addressed in the future. However, our proposed simulator and framework is still applicable and capable of taking these events into account in case they would be added in future research. Based on Table II, we can easily observe that all dynamic events impact the cost or demand of arcs. Therefore, we designed the *cost changer* and *demand changer* in our simulation system to simulate these events (Fig. 1).

¹<https://github.com/HawkTom/Dynamic-CARP>

TABLE II
TYPES OF DYNAMIC EVENTS IN DCARP. THE EVENTS WITH
* ARE NEW EVENTS CONSIDERED IN THIS ARTICLE, WHICH
HAVE NEVER BEEN CONSIDERED IN THE LITERATURE

Event types	Changes
1. Vehicle break down	Collection: $dm(u_k) : 0 \rightarrow Q - q_k$ Delivery: $dm(u_k) : \text{No change}$
2. Road closure	$dc(u) : \overline{dc(u)} \rightarrow \infty$
3. Congestion	$dc(u) : \overline{dc(u)} \rightarrow \overline{dc(u)} + c$
4. Recover from roads closure *	$dc(u) : \infty \rightarrow \overline{dc(u)}$
5. Recover from congestion *	$dc(u) : dc'(u) \rightarrow \overline{dc(u)}$
6. Congestion become worse *	$dc(u) : dc'(u) \rightarrow dc'(u) + c$
7. Congestion become better *	$dc(u) : dc'(u) \rightarrow dc'(u) - c$
8. Demand increases	$dm(u) : dm(u) \rightarrow dm(u) + d$
9. Added tasks	$dm(u) : 0 \rightarrow d$

$\overline{dc(u)}$ is the expected deadheading cost of arc u without congestion. $dc'(u)$ is the deadheading cost of arc u with congestion. c, d are the changing cost and demand, respectively. Event 5 is a special case of Event 7 where $c = dc'(u) - \overline{dc(u)}$ in Event 7.

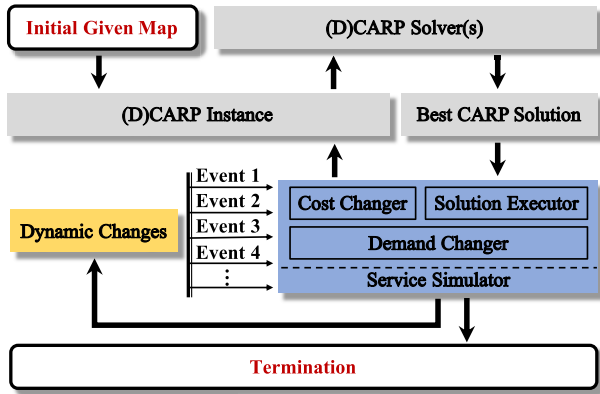


Fig. 1. Architecture of our simulation system.

In Fig. 1, the system starts from a provided initial graph, which could be taken from existing benchmarks for static CARP. Then, a CARP solver selected by the user, such as solvers based on memetic algorithms [6], can be used to obtain the initial solution, i.e., the first schedule for the vehicles. The core part of the system is the *service simulator* in Fig. 1, which is used to execute the CARP solution and update the graph. The pseudocode for the service simulator is presented in Algorithm 1. During the execution of the CARP solution, the maximum number of vehicles in the depot (N_{veh}) is considered. If the number of routes in the schedule exceeds the predefined maximum number of vehicles, the route with the smallest cost will be served first and the remaining routes will be served after some vehicles return to the depot. When the solution is executed, some dynamic events will happen according to a series of predefined parameters listed in line 1 and influence the graph at a uniformly random time between the service start and completion times. After that, a new DCARP instance is generated based on the dispatched solution. Different solutions will result in different DCARP instances, which might not facilitate fair comparison of different algorithms. Therefore, we apply the best solution among all solutions obtained by

Algorithm 1: Pseudocode of the Service Simulator

Input: Executable solution S , Previous instance I_m

Output: The new instance I_{m+1}

```

1 Set probabilities of occurrence for all events:
  [ $p_{event}, p_{road}, p_{bdr}, p_{crr}, p_{crbb}, p_{icd}, p_{add}$ ];
2 Execute  $S$  on  $I_m$ ;
3 Select a uniformly random time to stop execution;
4 Remove all served tasks: make demand of all served
  tasks be 0;
5 Event 1 Randomly select  $n$  vehicles to break down.
6 **** Cost Changer ****
7 for each arc  $u_i \in A$  do
8   if  $rand() < p_{event}$  then
9     switch state( $u_i$ ) do
10      case 0
11        if  $rand() < p_{road}$  then
12          Event 2  $dc(u_i) = \infty, state(u_i) = 2$ 
13        else
14          Event 3  $dc(u_i) = \overline{dc(u_i)} + c,$ 
15             $state(u_i) = 3$ 
16      case 2
17        if  $rand() > p_{bdr}$  then
18          Event 4  $dc(u_i) = \overline{dc(u_i)},$ 
19             $state(u_i) = 0$ 
20      case 3
21         $r = rand()$ 
22        if  $r < p_{crr}$  then
23          Event 5  $dc(u_i) = \overline{dc(u_i)},$ 
24             $state(u_i) = 0$ 
25        else if  $r < p_{crbb}$  then
26          Event 6  $dc(u_i) = dc'(u_i) + c$ 
27        else
28          Event 7  $dc(u_i) = dc'(u_i) - c$ 
29 **** Demand Changer ****
30 for each arc  $u_i \in A$  do
31   if  $dm(u_i) > 0$  and  $rand() < p_{icd}$  then
32     Event 8  $dm(u_i) = dm(u_i) + d$ 
33   if  $dm(u_i) == 0$  and  $rand() < p_{add}$  then
34     Event 9  $dm(u_i) = 0 + d$ 

```

different algorithms to the service simulator and generate one new DCARP instance for all algorithms for a fair comparison.

Once the dynamic change happens on the DCARP instance I_m , the service simulator stops the execution of the current solution. Then, the cost changer and demand changer will update the DCARP instance. First, as broken down vehicles influence only a specific arc, we simulate Event 1 separately from other dynamic events. The algorithm randomly selects n vehicles from all dispatched vehicles to break down, as shown in line 5. Events 2–7 will influence the cost of several arcs so that the cost changer mainly simulates these five events, as shown in lines 7–25. Each arc u_i has a traffic property,

$state(u_i)$, recording whether it is currently in a changed state compared to its original state having expected cost without traffic events.

In the cost changer, the simulator first determines whether or not a change from the current state occurs according to the probability p_{event} for each arc. If a change occurs, a dynamic event is triggered according to the events' probabilities and arc's current changed state. If an arc keeps the original state, i.e., $state(u_i) == 0$, Event 2 or 3 happens in this arc depending on probability p_{road} . If $state(u_i) == 2$, the road has broken down before so that it recovers with a probability p_{bdrv} . If $state(u_i) == 3$, the road is in congestion. It may either completely recover with a probability p_{crr} or the traffic jam may ease or get worse (by a random cost) with a probability p_{crbb} or $1 - p_{crbb}$, respectively. Compared to Events 2–7, Events 8 and 9 in the demand changer are much easier to implement, because we assume that the tasks/demands do not vanish unless served completely and the demand of tasks can only increase under the practical scenarios considered in this article. Event 8 may happen to a task with a probability p_{icd} , increasing the demand by a random amount. For arcs with no demand, Event 9 will happen with a probability p_{add} .

Finally, we will get a new DCARP instance I_{m+1} , and the solver generates a new DCARP solution. The system terminates after all tasks are served.

IV. GENERALIZED OPTIMIZATION FRAMEWORK FOR DCARP

In this section, we propose a virtual task (VT) strategy to change a DCARP instance to a “virtual static” instance. After that, a generalized optimization framework based on the VT strategy for DCARP with two different initialization strategies is proposed, which can make use of algorithms for static CARP for solving DCARP.

A. Virtual Task

As discussed in the previous section, the main challenge of scheduling vehicles for DCARP by using algorithms designed for static CARP is to take the outside vehicles with different locations and remaining capacities into account. We propose a VT strategy that forces all outside vehicles to virtually return to the depot for optimization purposes, such that all vehicles (some virtually) start at the depot during the optimization. As a result, algorithms for static CARP, which assume that all vehicles start at the depot, can be adopted. After the optimization, the obtained solution with routes starting from the depot will be converted to an executable solution according to the locations of outside vehicles. In other words, even though the outside vehicles will virtually return to the depot for running the optimization process, in the executable solutions themselves, the outside vehicles start their new routes from their outside locations. For this strategy to work, some adjustments need to be made so that the optimization problem with VTs is equivalent to the actual DCARP instance being solved. Such adjustments will be explained next.

The pseudocode of constructing the VT is presented in Algorithm 2. Despite virtually returning to the depot, the outside vehicles are still required to start from the stop location

Algorithm 2: Pseudocode of Constructing VTs

Input: Task set $R = \{t_1, t_2, \dots, t_{N_t}\}$,

Stop locations of outside vehicles: OV ,

Remaining capacity of outside vehicles: RQ .

$OV = \{v_1, v_2, \dots, v_{N_{ov}}\}$,

$RQ = \{q_1, q_2, \dots, q_{N_{ov}}\}$

Output: The updated task set: R

1 **for** each outside vehicle k **do**

2 Construct an Arc with virtual task vt_k ;

3 Head: $head_{vt_k} = v_0$, where v_0 is the depot;

4 Tail: $tail_{vt_k} = v_k$;

5 Deadheading cost: $dc(vt_k) = \infty$;

6 Serving cost: $sc(vt_k) = mdc(v_0, v_k)$;

7 Demand: $dm(vt_k) = Q - q_k$, where Q is the original capacity of vehicles;

8 Add this virtual task into task set: $R = R \cup vt_k$.

when executing the new schedule after a change. So, these virtually returned vehicles have to first virtually move to their stop location in the new schedule. Therefore, the vehicles must serve some virtual paths in the new schedule to reach this stop location. The graph of the CARP instance is thus modified to include these virtual paths, which can be regarded as VTs being optimized along with the normal tasks by a static CARP algorithm, as shown in lines 2–4. We also need all vehicles in the depot to have the same full capacities to be able to use static CARP algorithms. Therefore, we assign the previous demands that have been served by an outside vehicle to the corresponding VT, as shown in line 7. As a result, a DCARP instance is converted to a static CARP instance, in which all vehicles are located at the depot with the same capacities. It is worthy to mention that the VT idea has also been used for large-scale CARP [7], which is totally different from our idea here. They used the VT to represent the grouped neighboring tasks such that the problem's dimensionality can be reduced.

A VT can also be interpreted as a representation of an outside vehicle's previous serving status, including the total cost, served demand, and stop location before the occurrence of the dynamic events. During the optimization, the VTs are regarded as arcs to be assigned to routes when being rescheduled. These arcs need to be served, so that some depot vehicles will actually correspond to the outside vehicles. Once a depot vehicle serves a VT, its remaining capacity will become the same as the remaining capacity of the corresponding outside vehicle, and so will its stop location. However, vehicles that are not serving these virtual arcs should not be able to traverse them, because these virtual arcs are not actual physical paths that can be used by vehicles. This is achieved by assigning a deadheading cost (traversing cost) of $dc(vt) = \infty$ to these arcs, as shown in line 5. Note that this infinite traversing cost is not included as part of the serving cost.

The serving cost of a VT should be 0. This is because in reality, the outside vehicles are already in the stop locations and have already served some tasks. They should not incur any extra cost to stay where they were. However, in our strategy, a VT's serving cost is set as the minimal total deadheading

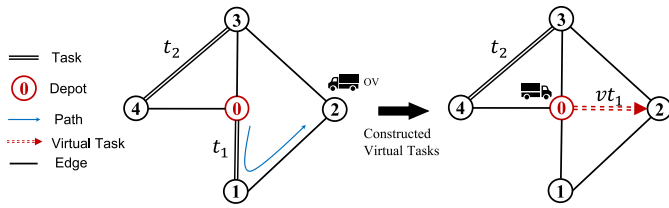


Fig. 2. Example of constructing VTs.

cost between the depot and the vehicle stop location (line 6) because some algorithms, such as path-scanning, use this cost as a denominator when deciding which task to assign to the current route [4]. To avoid this cost being counted toward the total cost in the objective function, the additional cost will be subtracted from the actual total cost after the optimization using the VT strategy. Besides, the demand is set as the amount corresponding to the demand already served by the vehicle, i.e., $Q - q_k$, to avoid the total demand of tasks in its new route exceeding the vehicle's remaining capacity q_k (line 7).

In order to improve the understanding of how VTs in DCARP instances are constructed, an example for tasks t_1 and t_2 is provided in Fig. 2. One vehicle traverses from v_0 (depot) and serves task t_1 (Fig. 2 left). When the dynamic change happens, a vehicle is located at v_2 . This vehicle is virtually placed into the depot and a VT vt_1 is constructed between v_0 and v_2 (Fig. 2 right). This VT will enable the vehicle to go back to its outside position to continue serving other tasks. The demand of vt_1 , $dm(vt_1)$, equals $Q - dm(t_1)$, such that when the vehicle virtually returns to its outside position, its remaining capacity will be the same as the remaining capacity at the rescheduling point. The deadheading cost of vt_1 , $dc(vt_1)$, is set to ∞ to prevent other vehicles from traversing the virtual arc. This enables the outside vehicle to serve the VT. The serving cost of vt_1 , $sc(vt_1)$, equals $mdc(v_0, v_2)$. This serving cost is incurred by the vehicle when it serves the VT, but is later on deducted from the objective function of the problem, so that the objective value with the VT strategy remains the same as the objective value without the VT strategy. After that, the new DCARP instance with the remaining task t_2 and the VT vt_1 will be optimized using one of the algorithms, which are available for static CARP, in which task t_1 is removed because it was already served before the change that triggered the rescheduling.

After applying the VT strategy, the route formulation in a DCARP solution $S = \{r_1, r_2, \dots, r_{N_{ov}}, \dots, r_K\}$ becomes

$$r_k = (v_0, vt_k, t_{k,2}, t_{k,3}, \dots, t_{k,l_k}, v_0), \quad k = 1, 2, \dots, N_{ov}.$$

$$r_k = (v_0, t_{k,1}, t_{k,2}, \dots, t_{k,l_k}, v_0), \quad k = N_{ov} + 1, \dots, K.$$

The new formulation of the optimization objective and the constraints for a DCARP instance is given as follows:

$$\begin{aligned} \text{Min } TC(S) &= \sum_{k=1}^K RC_{r_k} - \sum_{k=1}^{N_{ov}} mdc(v_0, v_k) \\ \text{s.t. } \sum_{k=1}^K l_k &= N_t + N_{ov} \end{aligned}$$

$$t_{k_1, i_1} \neq t_{k_2, i_2}, \text{ for all } (k_1, i_1) \neq (k_2, i_2)$$

$$\sum_{i=1}^{l_k} dm(t_{k,i}) \leq Q \quad \forall k = 1, \dots, K \quad (3)$$

where for route $\{r_k | k = 1, 2, \dots, N_{ov}\}$, $t_{k,1} = vt_k$. The second term $\sum_{k=1}^{N_{ov}} mdc(v_0, v_k)$ is to balance out line 6 in Algorithm 2 so that we do not count the serving costs of VTs.

The above adjustments enable a new schedule for the converted static CARP instance to be obtained by directly using metaheuristic algorithms for static CARP. An executable solution is obtained by removing the VTs from the routes in the new schedule and assigning it to the corresponding outside vehicles. The VT is better to be the first task in a vehicle's route. If a given VT is not the first task of a service route found by the static CARP algorithm, the tasks before this VT will be assigned to a new vehicle starting from the depot and the following tasks will be served by the corresponding outside vehicle. In such a case, we split a route that contains VTs in the middle into multiple routes with one route served by a vehicle from the depot and others served by the corresponding outside vehicle. In this way, the total cost of the CARP solution will not be influenced by splitting because the head node of the VT is also the depot. An example (without relations to Fig. 2) of converting an obtained new solution to an executable service plan is provided as follows:

$$\begin{aligned} &(v_0, vt_1, t_2, v_0), (v_0, t_3, t_4, vt_2, t_5, v_0) \\ &\quad \downarrow \\ &(v_0, vt_1, t_2, v_0), (v_0, t_3, t_4, v_0), (v_0, vt_2, t_5, v_0) \\ &\quad \downarrow \\ &(v_1, t_2, v_0), (v_0, t_3, t_4, v_0), (v_2, t_5, v_0). \end{aligned}$$

In the above example, the solution (top) contains two routes and two outside vehicles (i.e., two VTs). In the second route, the VT located in the middle of the task sequence. If the first task of a route is a VT, the remaining tasks of the route are served by the outside vehicle. Otherwise, all tasks of the route are served by a new empty vehicle. Therefore, after conversion (middle), tasks t_3 and t_4 are assigned to a new vehicle starting from the depot, but task t_5 should actually be served by the outside vehicle. The final executable routes (bottom), are obtained by removing the VTs and starting from the corresponding stop locations (v_1 and v_2 are the stop locations of outside vehicles corresponding to vt_1 and vt_2).

B. Proposed Framework Based on Virtual-Task Strategy

There are generally two commonly used strategies in dynamic optimization. One is to restart the optimization, which can also include some additional diversity enhancing techniques [28]. The other is to migrate some good solutions for the old environment to the new environment and initialize the starting individuals with them [29], [30].

These two strategies could also be used in our optimization framework. The RS is straightforward to apply after a change has occurred. However, the current strategies for reusing good solutions for the old environment may not be suitable for our DCARP scenarios because the dynamic events may influence

Algorithm 3: Pseudocode of Knowledge (Sequence) Transfer Strategy

Input: Previous best solution S_{m-1}
Output: A newly transferred solution S_m

- 1 Convert S_{m-1} into an ordered list of tasks P_{m-1} ;
- 2 Remove all served tasks from P_{m-1} ;
- 3 $P_m = P_{m-1}$, $l_p = |P_m|$;
- 4 The newly added tasks set $NT = \{nt_1, nt_2, \dots, nt_{|NT|}\}$;
- 5 **for** each $nt_i \in NT$ **do**
- 6 **for** each position in P_m **do**
- 7 Calculate the increased cost after insertion;
- 8 Obtain the position p with the smallest increased cost;
- 9 Insertion: $P_m = [t_1, \dots, t_p, nt_i, t_{p+1}, \dots, t_{l_p}]$;
- 10 $l_p = l_p + 1$;
- 11 $NT = NT \setminus \{nt_i\}$.
- 12 Use split scheme in P_m .

the problem's dimension and the previous solution's feasibility in a DCARP scenario. For example, the served tasks and added tasks change the total number of tasks, and the potential road closure event makes previous solutions infeasible in the new DCARP instance.

Therefore, we propose a new knowledge (especially, the sequence) transfer strategy for the DCARP scenario (Algorithm 3), which can benefit from previous DCARP instance's best solutions. Given an instance I_m , all scheduled routes in the best solution S_{m-1} of the previous instance I_{m-1} are concatenated to construct an ordered list of tasks P_{m-1} . All tasks that have been served are then removed from the list in P_{m-1} , and the remaining tasks keep their orders. After that, the newly added tasks are inserted into P_{m-1} greedily, i.e., they are inserted into the positions with the smallest increased cost. Finally, a corresponding transferred solution is generated by using the split scheme to convert an ordered list to an explicit-route solution. The newly transferred solution is used as one of the initial solutions when optimizing the new DCARP instance using the population-based algorithm.

On the basis of the VT strategy and two initialization strategies, i.e., the RS and the STS, we propose a generalized optimization framework with VTs (GOFVTs) to generalize static CARP algorithms to dynamic scenarios. Our framework comprises the following four main steps.

- 1) Construct VTs.
- 2) Apply the RS (randomly generate initial solutions) or the STS (generate one transferred solution for individual-based algorithms and additionally generated random solutions for population-based algorithms).
- 3) Apply the metaheuristic algorithm to optimize the converted static CARP instance.
- 4) Convert the obtained solution with VTs to an executable solution without VTs.

For a DCARP instance, the framework will first construct the VTs to convert the dynamic instance to a static instance. Then, one of the two initialization strategies explained above can be adopted to assist the optimization for the DCARP

instance. In the computational studies in Section V, we will compare the effectiveness of these two strategies. Then, metaheuristic algorithms with the initialization strategy are applied to optimize the DCARP instance, which is a static instance with VTs. Finally, the solution obtained for the static instance is converted into an executable solution, in which the routes with VTs are assigned to the corresponding outside vehicles and the routes without VTs are assigned to vehicles located at the depot.

V. COMPUTATIONAL STUDIES

In order to evaluate the efficiency of our proposed framework (GOFVT), three sets of experimental studies have been conducted by embedding a selection of metaheuristic algorithms in the GOFVT in this section. After providing the experimental setup (Section V-A), in the first experiment, the VT strategy is compared with a simple rescheduling strategy (Section V-B). After that, the VT strategy's efficiency is investigated by comparing it with an existing algorithm for DCARP in the second experiment (Section V-C). Finally, in the last experiment, GOFVT is combined with several classical metaheuristic algorithms originally designed for static CARP, and its performance is analyzed by running the newly generated algorithms in DCARP scenarios (Section V-D).

A. Experimental Settings

All experiments are conducted on a series of DCARP instances or scenarios generated by the simulation system presented in Section III-B, based on a static CARP benchmark, namely, the *egl* set [31]. The *egl* set contains 24 CARP instances. In each experiment, the DCARP instances or scenarios are generated independently from static CARP instances. For our first and second set of experiments, three DCARP instances are generated for each static CARP instance. These DCARP instances are not used to compose a DCARP scenario, as the algorithms just optimize the current instance and do not use any knowledge transfer in these two experiments. For the third experiment, one DCARP scenario including five DCARP instances is generated based on each CARP instance. For a fair comparison, each DCARP instance is generated from the best solution among all obtained solutions by all compared algorithms in the previous instance. When the simulator executes the selected solution according to the deployment policy, the time for serving all tasks will be calculated first and the simulator will uniformly randomly select a stop point (for dynamic events) within the longest time. As we only require a set of DCARP instances to test the effectiveness of the proposed strategies and framework, we have arbitrarily chosen parameters according to the real-world situations. For example, a road is more likely to become congested than being closed; hence, we set $p_{road} = 0.1$. In our experiments, the parameters of the simulator are chosen as $p_{event} = 0.5$, $p_{road} = 0.1$, $p_{bdrr} = 0.5$, $p_{err} = 0.3$, $p_{crbb} = 0.6$, $p_{cid} = 0.35$, and $p_{add} = 0.35$. In the future, we will carry out a more comprehensive study of the characteristics of simulator in relation to its parameter values. Eight different types of dynamic changes (Table II)

are simulated in our simulator excluding the case of “vehicles broken down” because its formulation is the same as the event of added tasks. As an illustrative example, we investigate the influence of different scenarios on the optimization algorithms’ performances. These examples show that the scenario with newly added tasks has a significant influence on the optimization algorithm’s performance.²

Because a key optimization requirement when dynamic changes happen in the real world is to obtain a new solution quickly, we limit the maximum optimization time to 60 s for the small problems (E1–E4) and 180s for larger maps (S1–S4) in *egl* for all algorithms. All programs are implemented in C language and run using a PC with an Intel Core i7-8700 3.2 GHz. The source code of our experiments has been available on github.³

B. Is It Necessary to Reschedule for DCARP?

Although many algorithms have been proposed to solve DCARP in the literature, a simple baseline strategy, named the return-first (RF) strategy, has been ignored. The RF strategy schedules all outside vehicles back to the depot first in order to convert a DCARP instance to a static one, and then reschedules all vehicles for the new static instance after all vehicles are located at the depot. If the RF strategy is efficient enough, the direct optimization of a DCARP instance would not be necessary any more. However, since this has not been shown in the literature so far, in this section, we use the proposed VT strategy to solve DCARP and compare it with the RF strategy to show the importance of optimizing DCARP instances directly instead of ignoring the outside vehicles and assigning new vehicles to all remaining tasks.

In our experiment, the simulation system generates three different DCARP instances for each test map (i.e., a static instance in the *egl* benchmark set) with different sets of remaining capacities. As this experiment aims to demonstrate the necessity and efficiency of directly optimizing DCARP instances, the setting of remaining capacities is divided into three intervals, i.e., $[0, 0.33Q]$, $[0.34Q, 0.66Q]$, and $[0.67Q, Q]$. Then, an optimization algorithm, memetic algorithm with extended neighborhood search (MANES) [6], assisted with the RF strategy and VT strategy are applied to optimize each DCARP instance, respectively. Two algorithm instantiations using MAENS follow the same setting during the optimization that the RF strategy and VT strategy is the only difference between them. The comparison results in terms of mean and standard deviation over 25 independent runs (mean \pm std), of the RF strategy and VT strategy on DCARP instances with different remaining capacities are presented in Table III. The bold values with the gray background for each DCARP instance are the better results between the RF strategy and VT strategy based on the Wilcoxon signed-rank test with a significance level of 0.05. The second-last row of Table III summarizes the number of win–draw–lose of the RF versus VT strategies. We have calculated the Wilcoxon signed-rank test with a significance level of 0.05 for the mean total cost of RF and VT strategies on the instances with the same range

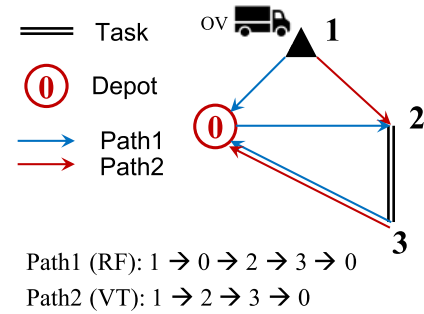


Fig. 3. Example of demonstrating why the RF strategy is not efficient enough when outside vehicles have enough remaining capacities.

of remaining capacities, and the p -values are listed in the last row of Table III.

Table III shows that the RF and VT strategies are significantly different for the instances, where the remaining capacities are in the range of $[0.34Q, Q]$ (instances 2 and 3 in Table III), with the VT strategy outperforming the RF strategy on all DCARP instances. In contrast, for the scenarios with remaining capacities in $[0, 0.33Q]$, there are 12 out of 24 DCARP instances, where the RF strategy outperforms the VT strategy. When comparing the results using the Wilcoxon test across maps, we confirm that none of these strategies is a consistent winner when analyzed across maps where the remaining capacities are smaller than $0.33Q$. This is understandable because when the vehicles are mostly fully loaded, i.e., when the remaining capacities are smaller than $0.33Q$, there is limited space for serving more tasks no matter what strategy is used.

In order to avoid the conclusion being biased by the employed metaheuristic algorithm, we have employed another metaheuristic algorithm, i.e., ILMA [32], to execute the same experiment. Due to the page limitation, we put the results into Table V of the supplementary material. The statistical analysis has confirmed the same conclusion as the experiments employing MAENS.

Overall, we can conclude that it is necessary and much more effective to optimize the DCARP instance directly rather than using the RF strategy when outside vehicles have enough remaining capacities.

The reason why the RF strategy is not always helpful when outside vehicles have enough remaining capacities can be explained using a simple example in Fig. 3, where an outside vehicle stops at vertex 1. If its remaining capacity is sufficient to serve task t_{23} , it can directly traverse from vertex 1 to vertex 2, presented as “Path 2” in Fig. 3, and the final total cost will be $d_{vt} = d_{12} + d_{23} + d_{30}$. But if we apply the RF strategy, the total cost will change to $d_{rf} = d_{10} + d_{02} + d_{23} + d_{30}$, presented as “Path 1” in Fig. 3. It is obvious that $d_{rf} \geq d_{vt}$ because $d_{10} + d_{02} \geq d_{12}$ according to the triangle inequality. The RF strategy increases the final cost because vehicles take a detour in such cases.

C. Analysis of the Effects of the Virtual-Task Strategy

MASDC [16] is the only metaheuristic algorithm for DCARP in the literature that considers a general DCARP

²More details are in Section IV and Table VI of the supplementary material.

³<https://github.com/HawkTom/Dynamic-CARP>

TABLE III

RESULTS OF VT STRATEGY AND RF STRATEGY ON DCARP INSTANCES WITH DIFFERENT SETTINGS OF REMAINING CAPACITIES FROM THE *egl* DATASET. THE VALUE IN EACH CELL REPRESENTS “MEAN \pm STD” OVER 25 INDEPENDENT RUNS AND THE BOLD ONES DENOTE THE BETTER RESULT ON THE DCARP INSTANCE BASED ON THE WILCOXON SIGNED-RANK TEST WITH A SIGNIFICANCE LEVEL OF 0.05. THE PENULTIMATE ROW SUMMARIES THE NUMBER OF WIN–DRAW–LOSE OF THE RF STRATEGY VERSUS VT STRATEGY AND THE LAST ROW PROVIDES THE p -VALUES OF THE WILCOXON SIGNED-RANK TEST WITH A SIGNIFICANCE LEVEL OF 0.05 ON INSTANCES WITH THE SAME SETTINGS OF ALL MAPS

Static Map	Instance 1 ($q \in [0, 0.33Q]$)		Instance 2 ($q \in [0.34Q, 0.66Q]$)		Instance 3 ($q \in [0.67Q, Q]$)	
	RF	VT	RF	VT	RF	VT
E1-A	8386 \pm 22	8095\pm31	10397 \pm 34	9925\pm22	8630 \pm 8	8566\pm10
E1-B	9830\pm29	9839\pm39	9718 \pm 22	8437\pm28	9675 \pm 16	9208\pm29
E1-C	12181\pm52	12109\pm52	14726 \pm 31	14106\pm16	11286 \pm 11	10565\pm25
E2-A	10255\pm6	10480 \pm 6	13740 \pm 27	12278\pm29	11692 \pm 51	10231\pm34
E2-B	13162\pm15	13317 \pm 23	16435 \pm 29	15207\pm18	15667 \pm 35	14321\pm55
E2-C	17425\pm41	17566 \pm 35	17444 \pm 32	16881\pm25	14186 \pm 16	13871\pm46
E3-A	11343 \pm 42	11167\pm17	12877 \pm 21	12030\pm26	10369 \pm 19	8869\pm12
E3-B	15517\pm84	15776 \pm 31	15150 \pm 31	12797\pm68	20743 \pm 59	20081\pm39
E3-C	20549\pm69	20880 \pm 63	20012 \pm 144	18078\pm88	27521 \pm 81	25289\pm82
E4-A	11216\pm31	11387 \pm 27	12489 \pm 26	12152\pm32	16213 \pm 29	14858\pm135
E4-B	15522 \pm 40	15242\pm62	14933 \pm 65	13791\pm63	17477 \pm 71	15869\pm29
E4-C	20928 \pm 63	20691\pm41	21998 \pm 28	20174\pm86	17869 \pm 79	15798\pm59
S1-A	16097 \pm 49	16012\pm40	15643 \pm 31	14917\pm40	13684 \pm 53	13159\pm18
S1-B	20462\pm69	21167 \pm 58	16184 \pm 35	15697\pm35	15151 \pm 19	13428\pm82
S1-C	27944\pm71	28624 \pm 116	21040 \pm 36	18616\pm87	26470 \pm 103	25789\pm76
S2-A	19610 \pm 85	19479\pm107	22314 \pm 40	20016\pm48	22499 \pm 67	19212\pm82
S2-B	27970\pm75	28408 \pm 59	26334 \pm 130	25911\pm118	25723 \pm 67	25024\pm94
S2-C	31859\pm108	32101 \pm 125	40170 \pm 132	38575\pm186	35053 \pm 143	31815\pm133
S3-A	19489 \pm 64	19211\pm107	23630 \pm 118	21329\pm98	28237 \pm 76	24494\pm71
S3-B	27518\pm72	27521\pm98	25651 \pm 64	24311\pm93	32286 \pm 50	30646\pm96
S3-C	32468 \pm 93	32049\pm107	35435 \pm 67	33927\pm68	43151 \pm 98	40801\pm97
S4-A	27256\pm87	28082 \pm 142	23780 \pm 74	22788\pm95	29895 \pm 102	27576\pm105
S4-B	34872 \pm 122	34709\pm149	28283 \pm 121	28023\pm93	31770 \pm 87	30652\pm125
S4-C	43746\pm168	44165 \pm 157	36808 \pm 117	36706\pm123	44006 \pm 145	42827\pm178
#of ‘w-d-l’	12-3-9		0-0-24		0-0-24	
p-value	0.22		1.82e-5		1.82e-5	

scenario including several dynamic events, such as road closure and added tasks. It comprises a distance-based split scheme (DSS) to assist the DCARP solution being used in the crossover and local search. Our VT strategy can convert a DCARP instance to a static CARP instance so that the operator used in the static CARP can be used in the DCARP instance directly. In this section, we analyze the effects of our VT strategy by embedding it to MASDC, referred to as VT-MASDC, and comparing it to the original MASDC. The advantage of embedding our strategy into MASDC is that this enables us to isolate and analyze the effect of the VTs compared to a state-of-the-art DCARP algorithm. In particular, all components in MASDC and VT-MASDC are the same except for the use of VTs and the DSS. The latter needs to be replaced by Ulusoy’s split scheme in VT-MASDC because the DSS is specifically designed for DCARP instances with outside vehicles at different stop locations. When we apply the VT strategy, the DCARP instance is converted to the static instance where all

vehicles are located at the depot. Therefore, the DSS is not suitable anymore and Ulusoy’s split scheme is used instead. The use of VTs is thus inherently linked to this split scheme, and any advantages provided by the VTs are also linked to the fact that they enable this split scheme to be adopted.

In our experiment, we generate three independent DCARP instances for each map in the *egl* benchmark set, ensuring that outside vehicles has enough remaining capacities, i.e., $q \geq 0.5Q$, in all generated instances. However, we need to generate DCARP instances rather than DCARP scenarios because the aim of DCARP is to minimize the total cost for each DCARP instance separately (2). The optimization results are presented in Table IV, in which the values in each cell represent the mean and standard deviation over 25 independent runs (mean \pm std). For each DCARP instance, the better result, based on the Wilcoxon signed-rank test with a significance level of 0.05, is highlighted using a bold font and gray background in Table IV. The summary of win–draw–lose of MASDC versus

TABLE IV

RESULTS OF MASDC AND VT-MASDC ON DCARP INSTANCES FROM THE *egl* DATASET. THE VALUE IN EACH CELL REPRESENTS MEAN \pm STD OVER 25 INDEPENDENT RUNS AND THE BOLD ONES DENOTE THE BETTER RESULT ON THE DCARP INSTANCE BASED ON THE WILCOXON SIGNED-RANK TEST WITH A SIGNIFICANCE LEVEL OF 0.05. THE LAST ROW SUMMARIZES THE NUMBER OF WIN-DRAW-LOSE OF MASDC VERSUS VT-MASDC

Map	Ins.Index	MASDC	VT-MASDC
S4-A	1	58456 \pm 1621	51512\pm3298
	2	55394 \pm 1746	49422\pm3517
	3	64795 \pm 1546	58676\pm3517
S4-B	1	64343 \pm 1886	57017\pm3622
	2	65027 \pm 1712	57413\pm3033
	3	60143 \pm 1612	53342\pm3323
S4-C	1	69224 \pm 1475	62760\pm2929
	2	68070 \pm 1424	62304\pm2465
	3	78134 \pm 1893	69348\pm3451
Statistical results over 72 instances below			
# of win-draw-lose		0-0-72	
p-value		1.67e-13	

The data of E1-A \sim S3-C are omitted in the table due to the page limitation. The complete data are provided in the supplementary material.

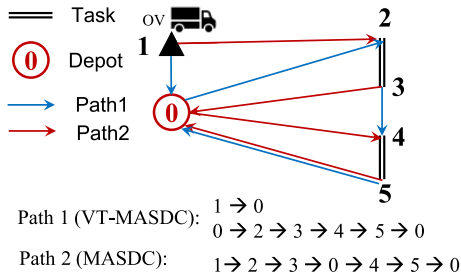


Fig. 4. Example of demonstrating the advantages of considering new vehicles.

VT-MASDC, which is presented in the last row, shows that VT-MASDC outperforms MASDC on all generated DCARP instances. The Wilcoxon signed-rank test with a significance level of 0.05 was conducted for the average total cost of VT-MASDC and MASDC in all instances, and the p -value was 1.67e-13. Overall, we can conclude that VT-MASDC performs much better than the original MASDC.

MASDC uses a DSS to evaluate DCARP solution's fitness because the split scheme designed for static CARP is not suitable for DCARP [25]. The DSS operator randomly splits the sequence of tasks to an executable CARP solution with explicit routes, and the random splitting process is repeated three times to obtain a better schedule. After embedding with the VT strategy, the DSS operator is replaced by Ulusoy's split [3] as explained in the beginning of this section, and the evaluation of a sequence of tasks only requires to apply Ulusoy's split once. As a result, the randomness brought by the DSS's split scheme is removed.

Moreover, the DSS operator never considers new vehicles starting from the depot during the optimization, whereas our VT strategy enables both outside and new vehicles to be used. We provide an example in Fig. 4 to show the advantages of

considering new vehicles during the optimization of DCARP. An outside vehicle is located at vertex 1, and its remaining capacity can only serve task t_{23} . We assume that $dd_{10} + dd_{02} \approx dd_{12}$ and $dd_{30} + dd_{04} \gg dd_{34}$ and the total cost of Path 1 and Path 2 can be calculated as

$$TC_1 = \underline{dd}_{10} + \underline{dd}_{02} + sc_{23} + \underline{dd}_{34} + sc_{45} + \underline{dd}_{50}$$

$$TC_2 = \underline{dd}_{12} + sc_{23} + \underline{dd}_{30} + \underline{dd}_{04} + sc_{45} + \underline{dd}_{50}.$$

For a sequence of tasks $[0, t_{23}, t_{45}, 0]$, if applied with the DSS operator, the only obtained path will be Path 2 as shown in Fig. 4. In contrast, if we use the VT strategy, a better path, i.e., Path 1 in Fig. 4, can be obtained, which avoids traversing the longer returning path.

D. Analysis of GOFVT

The proposed optimization framework GOFVT is capable of generalizing almost all algorithms for static CARPs to optimize DCARP. To demonstrate its effectiveness and efficiency, we have selected three classical metaheuristic algorithms for static CARPs, namely, RTS [33], ILMA [32], and MAENS [6], and embedded them into the GOFVT in our experiments to evaluate whether it is advantageous to make use of the existing static CARP algorithms within the GOFVT framework.

A brief description of each algorithm is presented as follows.

- 1) *RTS* [33]: A global repair operator which is embedded in a tabu search algorithm (TSA [5]). The source code is available online.⁴
- 2) *ILMA* [32]: An improved version of Lacomme's memetic algorithm (LMA) [1]. For our experiments, we implemented ILMA⁵ ourselves according to the details given in [32].
- 3) *MAENS* [6]: A memetic algorithm with a merge-split operator. The source code is available online.⁶

The newly generated algorithms for optimizing DCARP are denoted as VT-RTS, VT-ILMA, and VT-MAENS. We use these acronyms to denote GOFVT with the RS. When using the STS, they are denoted as VTtr-RTS, VTtr-ILMA, and VTtr-MAENS.

To demonstrate the efficiency and robustness of our proposed framework, we use parameters as given in their original papers [6], [32], [33]. In order to compare the restart and sequence transfer strategies, a DCARP scenario consisting of five DCARP instances has been generated for each static map in the *egl* benchmark set in our experiments. A new DCARP instance is generated by executing the obtained best solution of the previous DCARP instance in our simulation system.

We have also embedded MASDC into GOFVT and generated two algorithms as VT-MASDC and VTtr-MASDC, respectively. The results of above eight algorithms are presented in Table V. The values in each cell represent the mean \pm std and the average ranking (in the brackets) among eight algorithms in terms of the average total cost over 25

⁴<https://meiyi1986.github.io/publication/mei-2009-global/code.zip>

⁵<https://github.com/HawkTom/Dynamic-CARP>

⁶<https://meiyi1986.github.io/publication/tang-2009-memetic/code.zip>

TABLE V

RESULTS OF VT-RTS, VTTr-RTS, VT-ILMA, VTTr-ILMA, VT-MAENS, VTTr-MAENS, VT-MASDC, AND VTTr-MASDC ON THE *egl* DATASET. THE VALUES IN EACH CELL REPRESENT THE MEAN±STD WITH THE AVERAGE RANKING (IN THE BRACKETS) W.R.T THE AVERAGE TOTAL COST OVER 25 INDEPENDENT RUNS. THE BOLD VALUES ARE THE BETTER RESULTS UNDER THE WILCOXON SIGNED-RANK TEST WITH A SIGNIFICANCE LEVEL OF 0.05 BETWEEN RESTART AND INHERITING STRATEGIES IN AN ALGORITHM FOR A DCARP INSTANCE. THE LAST THREE ROWS SUMMARIZE THE NUMBER OF WIN–DRAW–LOSE OF RS VERSUS INHERITING STRATEGY IN EACH ALGORITHM AND THE *p*-VALUES OF THE WILCOXON SIGNED-RANK TEST WITH A SIGNIFICANCE LEVEL OF 0.05 ON ALL INSTANCES

Map	Ins.Index	VT-RTS	VTTr-RTS	VT-ILMA	VTTr-ILMA	VT-MAENS	VTTr-MAENS	VT-MASDC	VTTr-MASDC
S3-A	1	22989±156(3.6)	22971±190(3.4)	24100±307(5.5)	24073±289(5.5)	22411±61(1.5)	22401±70(1.5)	52327±3849(7.5)	52327±3849(7.5)
	2	25249±348(2.5)	26012±192(4.0)	27134±338(5.3)	27234±405(5.6)	25013±105(1.8)	25017±103(1.8)	57870±3931(7.5)	57870±3931(7.5)
	3	25907±350(3.3)	26117±160(3.7)	27011±250(5.5)	27042±320(5.5)	25285±145(1.4)	25349±113(1.6)	59652±3792(7.5)	59652±3792(7.5)
	4	41928±177(6)	33347±287(3)	34800±398(4.5)	34840±420(4.5)	32374±119(1.4)	32423±100(1.6)	72252±4788(7.5)	72250±4790(7.5)
	5	31319±4(6)	24329±316(2.7)	25614±322(4.6)	25632±334(4.4)	23989±74(1.7)	24006±85(1.6)	62362±4014(7.5)	62362±4014(7.5)
S3-B	1	30945±70(6)	29429±141(5)	26486±282(3.4)	26493±205(3.6)	25161±123(1.5)	25165±106(1.5)	46491±3247(7.5)	46491±3247(7.5)
	2	28494±1307(3.5)	29198±1867(4.1)	29318±356(5.2)	29374±347(5.2)	27445±121(1.8)	27356±140(1.2)	55642±2518(7.5)	55642±2518(7.5)
	3	36665±2093(5.3)	35529±3448(3.8)	34378±330(4.2)	34515±347(4.7)	32584±78(1.5)	32613±112(1.5)	65559±3265(7.5)	65559±3265(7.5)
	4	36424±10(6)	29498±240(3.0)	30262±280(4.6)	30306±339(4.4)	28983±133(1.6)	28930±131(1.4)	59740±4565(7.5)	59740±4565(7.5)
	5	32715±2377(4.0)	31524±348(3.7)	32271±345(5.2)	32185±417(5.1)	30444±167(1.4)	30437±160(1.6)	61165±3506(7.5)	61165±3506(7.5)
S3-C	1	45906±0(5.0)	47919±1147(6.0)	40932±333(3.4)	40930±425(3.6)	39026±146(1.4)	39049±154(1.6)	69270±3741(7.5)	69270±3741(7.5)
	2	58082±263(5.0)	58770±195(6.0)	51538±346(3.6)	51445±366(3.4)	49131±169(1.5)	49157±207(1.5)	78938±4233(7.5)	78938±4233(7.5)
	3	45802±74(5.2)	45868±21(5.8)	38727±341(3.4)	38925±241(3.6)	36791±118(1.6)	36730±94(1.4)	67602±3362(7.5)	67602±3362(7.5)
	4	41011±1(6)	40879±115(5)	35457±319(3.5)	35339±338(3.5)	33663±89(1.7)	33653±91(1.3)	61607±2949(7.5)	61607±2949(7.5)
	5	49309±114(5.5)	46793±3817(4.8)	42843±488(3.9)	42764±568(3.7)	40153±107(1.6)	40143±132(1.4)	72621±3858(7.5)	72621±3858(7.5)
S4-A	1	24849±1470(6)	21105±170(2.2)	22336±255(4.5)	22385±332(4.5)	20730±131(1.6)	20699±85(1.5)	53513±3603(7.5)	53513±3603(7.5)
	2	24693±1073(3.1)	24947±322(4.0)	26177±477(5.4)	26175±352(5.5)	23967±134(1.6)	23920±96(1.4)	59023±3019(7.5)	59020±3023(7.5)
	3	28262±12(6)	22203±286(3)	23181±356(4.4)	23091±319(5.4)	21661±67(1.6)	21638±68(1.4)	49301±3606(7.5)	49325±3575(7.5)
	4	28294±261(4.6)	27786±653(3.1)	28551±420(5.0)	28636±379(4.4)	26885±82(1.7)	26856±103(1.3)	62334±3972(7.5)	62334±3972(7.5)
	5	28727±249(3.0)	28989±389(3.6)	30571±479(5.5)	30693±441(5.5)	28421±139(1.6)	28440±125(1.8)	64233±5147(7.5)	64242±5138(7.5)
S4-B	1	47887±173(6)	40827±2573(3.3)	41301±476(4.4)	41242±464(4.4)	38564±117(1.6)	38549±139(1.4)	70139±4037(7.5)	70144±4029(7.5)
	2	43677±0(5.6)	43024±2961(4.7)	40667±448(3.7)	40804±492(4.0)	38055±128(1.5)	38061±172(1.5)	70219±3947(7.5)	70219±3947(7.5)
	3	50458±193(3.4)	50440±239(3.2)	52701±547(5.6)	52632±519(5.4)	50091±210(1.6)	50103±151(1.8)	83768±3444(7.5)	83768±3444(7.5)
	4	34946±288(5.6)	33974±1347(3.2)	34526±317(4.4)	34478±318(4.4)	32820±95(1.5)	32864±148(1.5)	62765±3949(7.5)	62765±3949(7.5)
	5	38698±4308(4.5)	38901±3107(4.8)	36166±349(4.4)	36195±289(4.4)	34049±163(1.6)	34016±143(1.4)	65365±4152(7.5)	65369±4147(7.5)
S4-C	1	42365±10(5.7)	42128±314(5.3)	35903±393(3.5)	35922±456(3.5)	33866±168(1.5)	33892±143(1.5)	61633±3417(7.5)	61633±3417(7.5)
	2	49614±26(5)	49797±74(6)	44052±394(3.4)	44087±340(3.6)	41842±170(1.4)	41878±204(1.6)	71240±3779(7.5)	71240±3779(7.5)
	3	50103±0(6)	49263±282(5)	41426±369(3.6)	41299±442(3.4)	39367±173(1.4)	39386±133(1.6)	71625±2776(7.5)	71625±2776(7.5)
	4	51311±0(6)	50781±48(5)	44940±369(3.4)	45099±410(3.6)	42895±168(1.4)	42939±179(1.6)	72347±3396(7.5)	72347±3396(7.5)
	5	46067±54(6)	45495±105(5)	40747±390(3.6)	40751±340(3.4)	38984±120(1.4)	38994±79(1.6)	66381±3802(7.5)	66381±3802(7.5)
Statistical results over 120 instances below									
	Avr.Ranking	5.25	4.78	3.95	4.00	1.51	1.51	7.50	7.5
	#of 'win-draw-lose'	43-18-59			4-116-0		1-118-1	0-120-0	
	<i>p</i> -value	0.01			0.15		0.93	0.95	

The data of E1-A ~ S2-C are omitted in the table due to the page limitation. The complete data has been attached as supplementary material.

independent runs. The bold values represent the better result between the RS and the STS for each algorithm on a DCARP instance under the Wilcoxon signed-rank test with a significance level of 0.05. Rows where both the RS and STS are in bold imply that these two strategies are not significantly different under the hypothesis test. The summaries of win–draw–lose of the RS versus the STS on all DCARP instances are listed in the penultimate row. We have also conducted the Wilcoxon signed-rank test with a significance level of 0.05 for the average total cost of the RS and STS of each metaheuristic algorithm on all instances, and the *p*-values associated with each metaheuristic algorithm are listed in the last row of Table V.

We conclude that the RS is significantly different from the STS when embedded in RTS (0.01 < 0.05), but both strategies obtain a similar performance when embedded in ILMA (0.15 > 0.05), MAENS (0.93 > 0.05), and MASDC (0.95 > 0.05). This is mainly because RTS is an individual-based metaheuristic algorithm while ILMA, MAENS, and MASDC are population-based algorithms. An individual-based algorithm only uses one solution during optimization. The solution generated by the STS will be the only initial solution in the individual-based algorithm and therefore significantly influences the optimization result. In contrast, the population-based algorithm contains a population during the optimization so that it depends much less on a single transferred solution.

From the statistical test result and the number of “win–draw–lose” of all DCARP instances for the individual-based algorithm, i.e., RTS, we can conclude that the performance of the STS is better than the RS. The efficiency depends on how much information is transferred from the previous best solution. For a CARP solution, the most critical information is the sequence of tasks of each route. Therefore, if each route has many tasks left, and these remaining tasks can also maintain the tasks’ sequence of the best solution in the previous instance, the transferred solution will be of high quality. The STS fixes the remaining tasks’ position to maintain the sequence information. Then, new tasks are inserted into the sequence to construct a new initial solution. If an outside vehicle has only a few remaining tasks, most tasks in the new schedule will be the new tasks so that the new schedule is unlikely to benefit much from the previous best schedule.

In contrast, if there are many remaining tasks for an outside vehicle, the order of remaining tasks will be maintained in the new sequence of tasks, and Ulusoy’s split will still assign them to an outside vehicle. Consider the following two remaining task sequences as an example:

$$S_1 : (v_0, vt_1, t_1, v_0, vt_2, t_2, vt_3, t_3, v_0)$$

$$S_2 : (v_0, vt_1, t_1, t_2, t_3, t_4, t_5, v_0, vt_2, t_6, t_7, t_8, t_9, t_{10}, t_{11}, v_0).$$

S_1 has three outside vehicles with one remaining task for each vehicle, and S_2 has two outside vehicles with five and

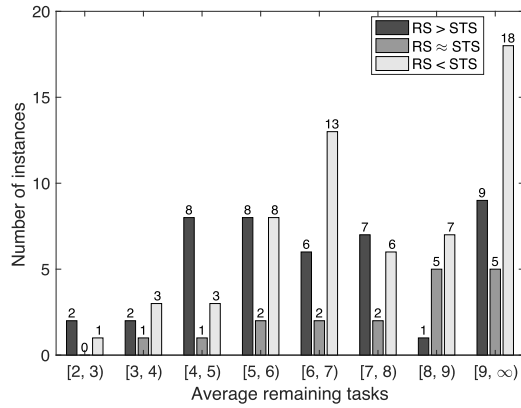


Fig. 5. Number of instances for the RS wins over (>), draws against (\approx), and loses to (<) the STS for different ranges of average remaining tasks.

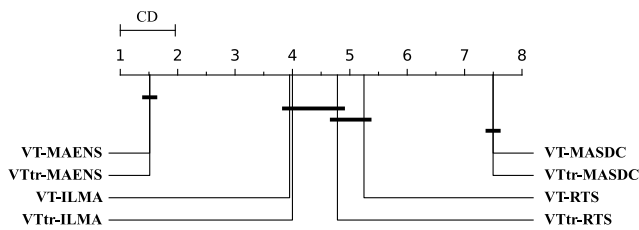


Fig. 6. Critical difference diagram for the comparison of eight algorithms against each other on *egl* with Friedman test and Nemenyi test. Groups of algorithms which are not significantly different at the level of 0.05 are connected.

six remaining tasks, respectively. The task sequences in both remaining task sequences are the same as those of the previous instance's best schedule. After greedy insertion of a set of new tasks, the final task sequence served by outside vehicles in S_2 will be more similar to the schedule in the previous instance's best solution. As a result, the second scenario is more likely to obtain a high-quality transferred solution.

We have calculated the average remaining tasks for outside vehicles on all DCARP instances in our experiment in Fig. 5. We can conclude that as the average remaining tasks for each outside vehicle increases, the STS benefits more from the optimization experience in the previous instance and outperforms the RS with a higher probability.

We also compared the rankings of each algorithm over 25 independent runs on each DCARP instance, which is presented in each cell's bracket in Table V. The overall average rankings of each algorithm instance over 120 DCARP instances are summarized in the row of "Avr. Ranking" in Table V. The Friedman test with a significance level of 0.05 was carried out to compare the ranking of eight algorithms across problem instances, leading to a p -value of $8.69e-159$. This indicates that at least one pair of algorithms are not equivalent to each other. We then perform the Nemenyi posthoc tests to identify which algorithms perform significantly different. The critical difference diagram is presented in Fig. 6, where the value of critical difference is 0.96 [34]. We can conclude from these results that the restart and sequence transfer strategies obtained almost the same performance for population-based algorithms (MAENS and ILMA) while the STS slightly outperformed

the RS in the individual-based algorithm (RTS) in our experiments.

Furthermore, MAENS obtains the best overall result, and RTS is the worst among the three metaheuristic algorithms, which are originally designed for static CARP. However, all of them significantly outperform the state-of-the-art dynamic algorithm, i.e., VT-MASDC and VTtr-MASDC. Recall that VT-MASDC was shown to outperform MASDC in Section V-C. Therefore, we can conclude that not only the proposed framework generalizes the existing algorithms for static CARPs to solve DCARPs but also that the constructed algorithm maintains its superior performance when optimizing a DCARP instance.

To evaluate the impact of parameter configuration of algorithms on our final conclusion, we have used SMAC [35] to obtain the best parameters for MAENS and MASDC, and then compared metaheuristic algorithms with tuned parameters on additional 72 DCARP instances. The results are presented in Table VII of the supplementary material. They show clearly that MASDC with tuned parameters still performed worse than MAENS with the default or tuned parameters. MAENS with tuned parameters performed similar to MAENS with default parameters in our experiments. In short, different parameter settings for the metaheuristic algorithms do not change our conclusions.

VI. CONCLUSION AND FUTURE WORK

In this article, we studied the DCARP, in which dynamic events, such as road closure, added tasks, etc., occur during the vehicles' service. First, a mathematical formulation of DCARP was provided for the first time in the literature. Then, we designed a simulation system as the research platform for DCARP. Unlike the existing benchmark generator, our simulation system generates DCARP instances from a given map in a way that is more realistic and closer to the real world. Our simulator also facilitates the use of existing algorithms for static CARP to be used for DCARP. The events simulated in our system enable the existing benchmark maps from static CARP to be adopted in dynamic scenarios much closer to the real world, where dynamic events happen while a solution is being deployed, i.e., while vehicles are serving in the map. Given the mathematical model and the simulation system, we have proposed a generalized optimization framework, which can generalize algorithms for static CARPs to optimize DCARPs. In our framework, we proposed a VT strategy that constructs a VT between the stop location and the depot, to make all outside vehicles virtually return to the depot, which tremendously simplified the optimization for DCARP. As a result, the DCARP instance was converted into a virtual static instance so that algorithms for static CARP can solve it.

Two initialization strategies were adopted in our generalized optimization framework: 1) the restart and 2) sequence transfer strategies. The RS completely restarts the optimization algorithm at random when there is a new DCARP instance. The STS maintains the sequence of remaining tasks to the new DCARP instance and greedily inserts the new tasks into

the remaining sequence, to transfer the information of task sequence from the previous optimization experience.

In our computational study, the necessity of directly optimizing DCARP together with outside vehicles was first demonstrated by comparing the VT strategy with an RF strategy. The results indicated that it would be more efficient to optimize the DCARP instance by using the VT strategy when the outside vehicles' remaining capacities were sufficiently large to serve more tasks. Then, the efficiency of the VT strategy was demonstrated by embedding it into an existing algorithm and comparing it to the original version of the existing algorithm. Finally, our generalized optimization framework's efficiency was analyzed by integrating a set of optimization algorithms that were designed for static CARPs, and the constructed algorithms performed significantly better than state-of-the-art algorithms for DCARP.

In this article, we have demonstrated that it is effective to solve DCARP instances by transforming them into static instances using the VT strategy and using our proposed GOFVT framework. The influence of the type and degree of dynamic events on individual optimization algorithms was not investigated. We will further investigate the influence of different dynamic events on optimization algorithms and design a benchmark including DCARP instances with different dynamic characteristics. Furthermore, the current STS only uses the optimization experience belonging to the instance of the previous optimization. It would be valuable to utilize all previous search experience taken from the whole DCARP scenario. Finally, it is desirable to test our proposed framework further with large-scale CARP instances and real world applications in the future.

REFERENCES

- [1] P. Lacomme, C. Prins, and W. Ramdane-Chérif, "Evolutionary algorithms for periodic arc routing problems," *Eur. J. Oper. Res.*, vol. 165, no. 2, pp. 535–553, 2005.
- [2] H. Handa, L. Chapman, and X. Yao, "Robust route optimization for gritting/salting trucks: A cercia experience," *IEEE Comput. Intell. Mag.*, vol. 1, no. 1, pp. 6–9, Feb. 2006.
- [3] G. Ulusoy, "The fleet size and mix problem for capacitated arc routing," *Eur. J. Oper. Res.*, vol. 22, no. 3, pp. 329–337, 1985.
- [4] B. L. Golden, J. S. DeArmon, and E. K. Baker, "Computational experiments with algorithms for a class of routing problems," *Comput. Oper. Res.*, vol. 10, no. 1, pp. 47–59, 1983.
- [5] J. Brandão and R. Eglese, "A deterministic tabu search algorithm for the capacitated arc routing problem," *Comput. Oper. Res.*, vol. 35, no. 4, pp. 1112–1126, 2008.
- [6] K. Tang, Y. Mei, and X. Yao, "Memetic algorithm with extended neighborhood search for capacitated arc routing problems," *IEEE Trans. Evol. Comput.*, vol. 13, no. 5, pp. 1151–1166, Oct. 2009.
- [7] K. Tang, J. Wang, X. Li, and X. Yao, "A scalable approach to capacitated arc routing problems based on hierarchical decomposition," *IEEE Trans. Cybern.*, vol. 47, no. 11, pp. 3928–3940, Nov. 2017.
- [8] S. Wöhlk and G. Laporte, "A fast heuristic for large-scale capacitated arc routing problems," *J. Oper. Res. Soc.*, vol. 69, no. 12, pp. 1877–1887, Jan. 2018.
- [9] M. C. Mourão and L. S. Pinto, "An updated annotated bibliography on arc routing problems," *Networks*, vol. 70, no. 3, pp. 144–194, Aug. 2017.
- [10] Á. Corberán, R. Eglese, G. Hasle, I. Plana, and J. M. Sanchis, "Arc routing problems: A review of the past, present, and future," *Networks*, vol. 77, no. 1, pp. 88–115, 2021.
- [11] L. Xing, P. Rohlfshagen, Y. Chen, and X. Yao, "An evolutionary approach to the multidepot capacitated arc routing problem," *IEEE Trans. Evol. Comput.*, vol. 14, no. 3, pp. 356–374, Jun. 2010.
- [12] R. K. Arakaki and F. L. Usberti, "Hybrid genetic algorithm for the open capacitated arc routing problem," *Comput. Oper. Res.*, vol. 90, pp. 221–231, Feb. 2018.
- [13] J.-M. Belenguer, E. Benavent, N. Labadi, C. Prins, and M. Reghioui, "Split-delivery capacitated arc-routing problem: Lower bound and metaheuristic," *Transp. Sci.*, vol. 44, no. 2, pp. 206–220, May 2010.
- [14] Y. Chen and J.-K. Hao, "Two phased hybrid local search for the periodic capacitated arc routing problem," *Eur. J. Oper. Res.*, vol. 264, no. 1, pp. 55–65, Jan. 2018.
- [15] J. de Armas, P. Keenan, A. A. Juan, and S. McGarraghy, "Solving large-scale time capacitated arc routing problems: From real-time heuristics to metaheuristics," *Ann. Oper. Res.*, vol. 273, nos. 1–2, pp. 135–162, Feb. 2018.
- [16] M. Liu, H. K. Singh, and T. Ray, "A memetic algorithm with a new split scheme for solving dynamic capacitated arc routing problems," in *Proc. IEEE Congr. Evol. Comput.*, 2014, pp. 595–602.
- [17] M. Liu, H. K. Singh, and T. Ray, "A benchmark generator for dynamic capacitated arc routing problems," in *Proc. IEEE Congr. Evol. Comput.*, 2014, pp. 579–586.
- [18] Y. Mei, K. Tang, and X. Yao, "Evolutionary computation for dynamic capacitated arc routing problem," in *Evolutionary Computation for Dynamic Optimization Problems*. Heidelberg, Germany: Springer, 2013, pp. 377–401.
- [19] J. Liu, K. Tang, and X. Yao, "Robust optimization in uncertain capacitated arc routing problems: Progresses and perspectives," *IEEE Comput. Intell. Mag.*, vol. 16, no. 1, pp. 63–82, Feb. 2021.
- [20] H. Handa, L. Chapman, and X. Yao, "Dynamic salting route optimisation using evolutionary computation," in *Proc. IEEE Congr. Evol. Comput.*, vol. 1, 2005, pp. 158–165.
- [21] M. Tagmouti, M. Gendreau, and J.-Y. Potvin, "A dynamic capacitated arc routing problem with time-dependent service costs," *Transp. Res. C Emerg. Technol.*, vol. 19, no. 1, pp. 20–28, 2011.
- [22] M. Monroy-Licht, C. A. Amaya, A. Langevin, and L.-M. Rousseau, "The rescheduling arc routing problem," *Int. Trans. Oper. Res.*, vol. 24, no. 6, pp. 1325–1346, 2017.
- [23] W. Padungwech, J. Thompson, and R. Lewis, "Effects of update frequencies in a dynamic capacitated arc routing problem," *Networks*, vol. 76, no. 4, pp. 522–538, 2020.
- [24] A. Yazici, G. Kirlik, O. Parlaktuna, and A. Sipahioglu, "A dynamic path planning approach for multi-robot sensor-based coverage considering energy constraints," in *Proc. IEEE/RSJ Int. Conf. Intell. Robots Syst.*, 2009, pp. 5930–5935.
- [25] H. Tong, L. L. Minku, S. Menzel, B. Sendhoff, and X. Yao, "Towards novel meta-heuristic algorithms for dynamic capacitated arc routing problems," in *Proc. Int. Conf. Parallel Problem Solving Nat.*, 2020, pp. 428–440.
- [26] V. Pillac, M. Gendreau, C. Guéret, and A. L. Medaglia, "A review of dynamic vehicle routing problems," *Eur. J. Oper. Res.*, vol. 225, no. 1, pp. 1–11, 2013.
- [27] L. Foulds, H. Longo, and J. Martins, "A compact transformation of arc routing problems into node routing problems," *Ann. Oper. Res.*, vol. 226, no. 1, pp. 177–200, Sep. 2014.
- [28] M. Mavrouniotis, C. Li, and S. Yang, "A survey of swarm intelligence for dynamic optimization: Algorithms and applications," *Swarm Evol. Comput.*, vol. 33, pp. 1–17, Apr. 2017.
- [29] T. T. Nguyen, S. Yang, and J. Branke, "Evolutionary dynamic optimization: A survey of the state of the art," *Swarm Evol. Comput.*, vol. 6, pp. 1–24, Oct. 2012.
- [30] M. Mavrouniotis and S. Yang, "Adapting the pheromone evaporation rate in dynamic routing problems," in *Proc. Eur. Conf. Appl. Evol. Comput.*, 2013, pp. 606–615.
- [31] L. Y. Li and R. W. Eglese, "An interactive algorithm for vehicle routing for winter—Gritting," *J. Oper. Res. Soc.*, vol. 47, no. 2, pp. 217–228, 1996.
- [32] Y. Mei, K. Tang, and X. Yao, "Improved memetic algorithm for capacitated arc routing problem," in *Proc. IEEE Congr. Evol. Comput.*, 2009, pp. 1699–1706.
- [33] Y. Mei, K. Tang, and X. Yao, "A global repair operator for capacitated arc routing problem," *IEEE Trans. Syst., Man, Cybern. B, Cybern.*, vol. 39, no. 3, pp. 723–734, Jun. 2009.
- [34] J. Demšar, "Statistical comparisons of classifiers over multiple data sets," *J. Mach. Learn. Res.*, vol. 7, pp. 1–30, Dec. 2006.
- [35] F. Hutter, H. H. Hoos, and K. Leyton-Brown, "Sequential model-based optimization for general algorithm configuration," in *Proc. Int. Conf. Learn. Intell. Optim.*, 2011, pp. 507–523.



Hao Tong (Member, IEEE) received the B.E. degree from the China University of Mining and Technology, Xuzhou, China, in 2017, and the M.A.Sc. degree from the Joint Program of the Southern University of Science and Technology, Shenzhen, China, and the Harbin Institute of Technology, Harbin, China, in 2019. He is currently pursuing the Ph.D. degree with the University of Birmingham, Birmingham, U.K.

His research interests include metaheuristic algorithm, arc routing problem, dynamic optimization, and surrogate-assisted evolutionary algorithm.



Leandro L. Minku (Senior Member, IEEE) received the Ph.D. degree in computer science from the University of Birmingham, Birmingham, U.K., in 2010.

He is an Associate Professor with the School of Computer Science, University of Birmingham. Prior to that, he was a Lecturer of Computer Science with the University of Leicester, Leicester, U.K., and a Research Fellow with the University of Birmingham. His main research interests include machine learning for nonstationary environments/data stream mining, class-imbalanced learning, ensembles of learning machines, dynamic optimization, and computational intelligence for software engineering.

Dr. Minku is an Associate Editor-in-Chief of *Neurocomputing* and an Associate Editor of *IEEE TRANSACTIONS ON NEURAL NETWORKS AND LEARNING SYSTEMS*, *Empirical Software Engineering*, and *Journal of Systems and Software*.



Stefan Menzel received the Dipl.-Ing. degree in civil engineering from RWTH Aachen, Aachen, Germany, in 1998, and the Ph.D. degree in civil engineering from Technical University Darmstadt, Darmstadt, Germany, in 2004.

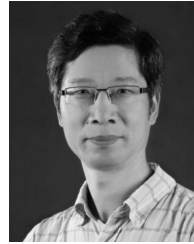
Since 2004, he has been with the Honda Research Institute Europe GmbH, Offenbach, Germany, where he is currently a Chief Scientist with the Optimization and Creativity Group. His current research interests include evolutionary optimization with special focus on adaptive representations, machine learning for knowledge transfer, and multidisciplinary optimization for real-world applications.



Bernhard Sendhoff (Fellow, IEEE) received the diploma degree in theoretical physics and the Ph.D. degree in applied physics (Artificial Intelligence) from the Ruhr-Universität Bochum, Bochum, Germany, in 1993 and 1998, respectively.

After working with Honda R&D Europe (Deutschland) GmbH, Offenbach, Germany, from 1999 to 2003, he was working as a Chief Technology Officer of Honda Research Institute Europe GmbH, Offenbach, from 2003 to 2011 and as the President from 2011 to 2018. From 2017 to 2021, he was the Head of Global Operations of the Honda Research Institutes and from 2019 to 2021, he was the President of Honda Research Institute Japan Co., Ltd., Saitama, Japan. From 2007 to 2020, he was an Honorary Professor with the School of Computer Science, University of Birmingham, Birmingham, U.K. Since 2017, he has been an Operating Officer of Honda R&D Co., Ltd., Tokyo, Japan. Since 2021, he has been a Chief Executive Officer of the Global Network Honda Research Institutes and since 2008, he has been an Honorary Professor with the Technical University of Darmstadt, Darmstadt, Germany. Since 2011, he has been the Managing Director of the Honda Research Institute Europe GmbH. He has authored or coauthored more than 190 peer-reviewed journal and conference papers and over 40 patents. He has an h-index of 48 (Google Scholar).

Dr. Sendhoff has been an Associate Editor of the *IEEE TRANSACTIONS ON EVOLUTIONARY COMPUTATION* since 2006 and since 2017, he has been an Associate Editor for the *IEEE TRANSACTIONS ON COGNITIVE AND DEVELOPMENTAL SYSTEMS*. He is a Senior Member of ACM and a member of SAE.



Xin Yao (Fellow, IEEE) received the B.Sc. degree from the University of Science and Technology of China (USTC), Hefei, China, in 1982, the M.Sc. degree from the North China Institute of Computing Technologies, Beijing, China, in 1985, and the Ph.D. degree from USTC, in 1990.

He is a Chair Professor and the Founding Head of Computer Science and Engineering with the Southern University of Science and Technology, Shenzhen, China, and a Part-Time Professor of Computer Science with the University of Birmingham, Birmingham, U.K. His major research interests include evolutionary computation and ensemble machine learning. In particular, he is very interested in metaheuristics for dynamic optimization and capacitated arc routing problems.

Dr. Yao's work won the 2001 IEEE Donald G. Fink Prize Paper Award; the IEEE TRANSACTIONS ON EVOLUTIONARY COMPUTATION Outstanding Paper Awards in 2010, 2016, and 2017; the 2011 IEEE TRANSACTIONS ON NEURAL NETWORKS Outstanding Paper Award; the 2010 BT Gordon Radley Award for the Best Author of Innovation (Finalist); and several best paper awards at conferences. He received the 2012 Royal Society Wolfson Research Merit Award, the 2013 IEEE CIS Evolutionary Computation Pioneer Award, and the 2020 IEEE Frank Rosenblatt Award. He was a Distinguished Lecturer of the IEEE Computational Intelligence Society (CIS). He served as the President from 2014 to 2015 of IEEE CIS and the Editor-in-Chief of *IEEE TRANSACTIONS ON EVOLUTIONARY COMPUTATION* from 2003 to 2008.